Technology in Cancer Research & Treatment
Volume 19: 1-10

DOI: 10.1177/1533033820928073
journals.sagepub.com/home/tct
SAGE

Sodium Tanshinone IIA Sulfonate Attenuates Tumor Oxidative Stress and Promotes Apoptosis in an Intermittent Hypoxia Mouse Model

Xiao-Bin Zhang, PhD[1], Xiao-Yang Chen, PhD[2], Peng Sun, MD[1], Xiao-Man Su, Nurse[1], Hui-Qing Zeng, PhD[1], Yi-Ming Zeng, PhD[2], Miao Wang, MD[1], and Xiongbiao Luo, PhD[3]

Abstract

Objective: Intermittent hypoxia, a significant feature of obstructive sleep apnea, has pro-tumorigenic effects. Here, we investigated the effect of sodium tanshinone IIA sulfonate on oxidative stress and apoptosis in a mouse model of Lewis lung carcinoma with intermittent hypoxia. **Methods:** Mice were randomly assigned to normoxia (control), normoxia plus sodium tanshinone IIA sulfonate (control + sodium tanshinone IIA sulfonate), intermittent hypoxia, and intermittent hypoxia + sodium tanshinone IIA sulfonate groups. Intermittent hypoxia administration lasted 5 weeks in the intermittent hypoxia groups. Lewis lung carcinoma cells were injected into the right flank of each mouse after 1 week of intermittent hypoxia exposure. Sodium tanshinone IIA sulfonate was injected intraperitoneally in the control + sodium tanshinone IIA sulfonate and intermittent hypoxia + sodium tanshinone IIA sulfonate groups. Tumor oxidative stress was evaluated by detection of malondialdehyde and superoxide dismutase. The apoptosis of tumor cells was evaluated by the terminal deoxynucleotidyl transferase dUTP nick-end labeling assay as well as by Western blot analysis of B-cell lymphoma 2-associated X protein and cleaved caspase-3 expression. Additionally, the expression of hypoxia-induced factor-1α, nuclear factor erythroid 2-related factor 2, and nuclear factor kappa B was also evaluated by Western blot. **Results:** Compared with the control group, the intermittent hypoxia treatment significantly increased Lewis lung carcinoma tumor growth and oxidative stress (serum malondialdehyde) but decreased serum levels of SOD and pro-apoptotic markers (terminal deoxynucleotidyl transferase dUTP nick-end labeling staining, B-cell lymphoma 2-associated X protein, and cleaved caspase-3). These changes were significantly attenuated by intraperitoneal injection of sodium tanshinone IIA sulfonate. Lower nuclear factor erythroid 2-related factor 2 and higher nuclear factor kappa B levels in the intermittent hypoxia group were clearly reversed by sodium tanshinone IIA sulfonate treatment. In addition, sodium tanshinone IIA sulfonate administration decreased the high expression of hypoxia-induced factor-1α induced by intermittent hypoxia. **Conclusion:** Intermittent hypoxia treatment resulted in high oxidative stress and low apoptosis in Lewis lung carcinoma–implanted mice, which could be attenuated by sodium tanshinone IIA sulfonate administration possibly through a mechanism mediated by the nuclear factor erythroid 2-related factor 2/nuclear factor kappa B signaling pathway.

Keywords

intermittent hypoxia, tumor, sodium tanshinone IIA sulfonate, oxidative stress, apoptosis

[1] Department of Pulmonary and Critical Care Medicine, Zhongshan Hospital, Xiamen University, Teaching Hospital of Fujian Medical University, Siming District, Xiamen, Fujian Province, People's Republic of China
[2] Department of Pulmonary and Critical Care Medicine, Second Clinical Medical College of Fujian Medical University, the Second Affiliated Hospital of Fujian Medical University, Center of Respiratory Medicine of Fujian Province, People's Republic of China
[3] Department of Computer Science, Xiamen University, Xiamen, Fujian, People's Republic of China

Corresponding Authors:
Xiao-Bin Zhang and Hui-Qing Zeng, Department of Pulmonary and Critical Care Medicine, Zhongshan Hospital, Xiamen University, Teaching Hospital of Fujian Medical University, No.201, Hubin Nan Road, Siming District, Xiamen, Fujian Province, People's Republic of China, 361004.
Emails: zhangxiaobincn@xmu.edu.cn; zhq20071212@xmu.edu.cn

Abbreviations

BAX, B-cell lymphoma 2-associated X protein; CTL, control; HIF-1α, hypoxia-induced factor-1α; IH, intermittent hypoxia; KO, knockout; LLC, Lewis lung carcinoma; MDA, malondialdehyde; NF-κB, nuclear factor kappa B; Nrf2, nuclear factor erythroid 2-related factor 2; OSA, obstructive sleep apnea; PBS, phosphate-buffered saline; PVDF, polyvinylidene fluoride; qPCR, quantitative polymerase chain reaction; ROS, reactive oxygen species; SOD, superoxide dismutase; TBST, Tris-buffered saline, 0.1% Tween-20; TSA, sodium tanshinone IIA sulfonate; TUNEL, terminal deoxynucleotidyl transferase dUTP nick-end labeling

Received: July 07, 2019; Revised: March 27, 2020; Accepted: April 16, 2020.

Introduction

Sodium tanshinone IIA sulfonate (TSA) is a natural compound extracted from the Chinese herb *Salvia miltiorrhiza*. Previous studies have indicated that TSA has antioxidant and anti-inflammatory effects through reduction of reactive oxygen species (ROS) production and alleviation of pro-inflammatory cytokines.[1,2] Studies have shown that TSA is extensively applied for cardiovascular disease and inflammatory disorders, such as chronic hepatitis.[3,4] Recent *in vitro* studies revealed the anticancer activity of TSA in many cancer types including lung cancer, leukemia, liver cancer, and gastric cancer.[5-8] Indeed, an *in vivo* study also verified the anticancer activity of TSA.[9] The anticancer effects of TSA may be partly attributed to its antioxidant and proapoptotic properties.[6,9]

Obstructive sleep apnea (OSA) is a disorder with high global prevalence (15% to 24%).[10-12] Obstructive sleep apnea is characterized by recurrent cycles of intermittent hypoxia (IH), which contributes to systematic inflammation, oxidative stress, endothelial dysfunction, and apoptosis.[13,14] During the last decade, a considerable amount of literature has shown a higher cancer incidence and mortality in OSA patients.[15,16] In addition, a study by our group and others demonstrated that IH induced tumor growth, invasion, and metastasis in mouse models of sleep apnea.[17-20]

Based on the abovementioned findings, we hypothesized that oxidative stress and apoptosis may play important roles in the pathogenesis of cancer progression accelerated by IH. Sodium tanshinone IIA sulfonate has antioxidative activity that partially attenuates OSA-induced tumor growth. Thus, the aim of this study was to assess the effects and underlying molecular mechanisms of TSA on tumor oxidative stress and apoptosis in an IH mouse model mimicking OSA.

Materials and Methods

Animals and Groups

Forty-eight 7-week-old male C57BL/6 mice were purchased from the Chinese Academy of Science Laboratory Animals Center (Shanghai, China). All mice were housed in standard cages with a 12:12-hour light-dark cycle and free access to water and food. Mice were randomly assigned to the following groups (n = 12 in each group): normoxia (control, CTL), control plus TSA (CTL + TSA), IH, and IH plus TSA (IH + TSA). The body weight of the mice in each group was measured every week.

Ethical Approval

The study protocol was approved by the ethics committee of Zhongshan Hospital, Xiamen University (approval no. 2017-015) and conducted in accordance with the Guide for the Care and Use of Laboratory Animals.[21]

IH Exposure

Intermittent hypoxia exposure was conducted as described previously.[20,22-24] Briefly, mice in the IH and IH + TSA groups (n = 24) were placed in a self-made plexiglass chamber with 1-way valves in which the gas flow of oxygen, nitrogen, and compressed air was controlled by a program to enable alteration of the oxygen concentration from 21% to nadir 6% to 8%. The cycle time of hypoxia (6% to 8%) and reoxygenation (21%) was 120 seconds. Intermittent hypoxia exposure was conducted from 8:00 AM to 4:00 PM daily for 5 consecutive weeks.

Cell Culture, Tumor Implantation, and Measurement

Lewis lung carcinoma (LLC) cells (CoBioer Biosciences) were cultured according to the manufacturer's instructions. Briefly, LLC cells were maintained in high-glucose Dulbecco's Modified Eagle's Medium and supplemented with 10% fetal bovine serum (Gibco). A total of 1×10^6 LLC cells in 100-μL phosphate-buffered saline (PBS) were subcutaneously injected into the right flank of each mouse in week 1 of the experiment. When the tumor was palpable, its width (W) and length (L) were recorded with an electric caliper weekly. Tumor volume (V, mm^3) was calculated as $W^2 \times L/2$.

Drug Administration

Once tumor volume reached approximately 200 mm^3 (about 5-7 days after LLC injection), mice in the CTL + TSA and IH + TSA groups were intraperitoneally injected daily with TSA (10 mg/kg; Shanghai No.1 Biochemical & Pharmaceutical).[2,25-27] Meanwhile, mice in the CTL and IH groups were intraperitoneally injected with the same volume of saline.

Table 1. Primers Used in the RT-PCR Analysis.

Primer name	Forward	Reverse
HIF-1α	CGACCACTGCTAAGGCATCA	AGTGGCAGACAGGTTAAGGC
β-actin	CCACTGCCGCATCCTCTTCC	CTCGTTGCCAATAGTGATGACCTG

Abbreviation: RT-PCR, reverse transcription polymerase chain reaction.

Serum and Tissue Sample Preparation from LLC-Implanted Mice

At 5 weeks after LLC implantation, all mice were deeply anesthetized with pentobarbital and exsanguinated by cardiac puncture, after which plasma was isolated. After excision and weighing, the tumors were either frozen in liquid nitrogen/ −80 °C freezer (for further analysis) or fixed in buffered 10% formalin for histological examination.

Oxidative Stress Measurement

Two of the most common indicators of oxidative stress, malondialdehyde (MDA) and superoxide dismutase (SOD), were assayed using relevant kits according to the manufactures' instructions (Catalog numbers: S0131 and S0087; Beyotime Biotechnology). Briefly, the frozen tumor tissue samples were homogenized with a 5-mL glass Potter-Elvehjem homogenizer in ice-cold PBS (10% Wt/Vol).[22,28] After lysis for 15 minutes on ice, the homogenates were centrifuged and the supernatants were obtained for further investigation. Malondialdehyde concentration in the homogenates was determined spectrophotometrically by measuring the presence of thiobarbituric acid reactive substances (utilizing the principle of the thiobarbituric acid colorimetric method).[29,30] Superoxide dismutase was detected by a corresponding assay kit based on the principle of the WST-8 colorimetric reaction, which employs a thiazole salt for detection of superoxide anions by producing a colored product. The amount (mg) of enzyme that transformed 1-μmol substrate (superoxide radical for SOD) in 1 minute was defined as 1 enzyme activity unit. The absorbance of the MDA and SOD assays was measured at wavelengths of 535 and 560 nm, respectively.

Quantitative Polymerase Chain Reaction

TRIzol reagent (Invitrogen) was used for total messenger RNA extraction from the tumors, according to the manufacturer's instructions (TakaRa Biotechnology). Then 2-mg total RNA was reverse-transcribed using TaqMan MicroRNA Reverse Transcription Kit (Thermo Fisher Scientific) to obtain the first-strand complementary DNA. Next, 1 μL of the complementary DNA was applied as template for the quantitative polymerase chain reaction (qPCR) using SYBR Green PCR reagent kit (Toyobo Co) in the Applied Biosystems 7500 Fast Real-Time PCR System (Applied Biosystems) under the following conditions: 95 °C for 30 seconds, followed by 40 cycles at 95 °C for 3 seconds and 60 °C for 30 seconds. The primers used in the qPCR reactions are outlined in Table 1. The relative gene expression levels were calculated with $2^{-\Delta\Delta Ct}$. β-Actin was used as the internal reference.

Western Blot Analysis

Tumor tissues were homogenized with RIPA buffer (Beyotime) containing protease and phosphatase inhibitors in a glass homogenizer. After centrifugation, the supernatants were extracted and total protein concentration was measured with the bicinchoninic acid protein assay (Beyotime). Then the proteins were resolved on 12% sodium dodecyl sulfate polyacrylamide gel electrophoresis gels (40 μg/lane) and electrotransferred onto polyvinylidene fluoride (PVDF) membranes (Millipore). After blocking in 5% (Wt/Vol) skim milk, the membrane was incubated with the following antibodies at 4 °C overnight: mouse anti-hypoxia-induced factor-1α (HIF-1α) monoclonal antibody (1:250; Novus Biologicals), rabbit anti-B-cell lymphoma 2-associated protein X (BAX;1:1000; Cell Signaling Technology [CST]), rabbit anti-cleaved caspase-3 (1:1000; CST), rabbit antinuclear factor erythroid 2-related factor 2 (Nrf2; 1:2000; Abcam), rabbit antinuclear factor kappa B (NF-κB) p65 (1:1000; CST), rabbit anti-phosphorylated NF-κB (*p*-NF-κB) p65 (1:1000; CST), or mouse anti-β-actin (1:2000; Santa Cruz Biotechnology). After rinsing 3 times with Tris-buffered saline, 0.1% Tween-20 (TBST), the PVDF membranes were incubated with goat anti-rabbit or goat anti-mouse IgG horseradish peroxidase-conjugated antibody (1:10000; Santa Cruz Biotechnology) at 37 °C for 1 hour. After 3 washes with TBST, the membranes were developed using an enhanced chemiluminescence kit (Clarity Western ECL Substrate; Bio-Rad). The protein bands were visualized using ImageQuant LAS 400 Mini (GE Healthcare Life Sciences). Each experiment was repeated in triplicate. Densitometry was done using Image J analysis software (National Institutes of Health).

Terminal Deoxynucleotidyl Transferase dUTP Nick-End Labeling Assay

Tumor tissues were fixed in 10% formalin for 24 hours, dehydrated in graded series of alcohol, cleaned with xylene, and then embedded in paraffin. The embedded tissues were sectioned to 5 μm, placed on glass slides, and washed with PBS. Then the terminal deoxynucleotidyl transferase dUTP nick-end labeling (TUNEL) assay was performed at 37 °C for 1 hour using the In Situ Cell Death Detection Kit (Roche). After washing with PBS and incubation with 4′, 6-diamidino-2-phenylindole (Sigma) for 5 minutes, the TUNEL-stained cells were analyzed and photographed with a microscope (SPII2-

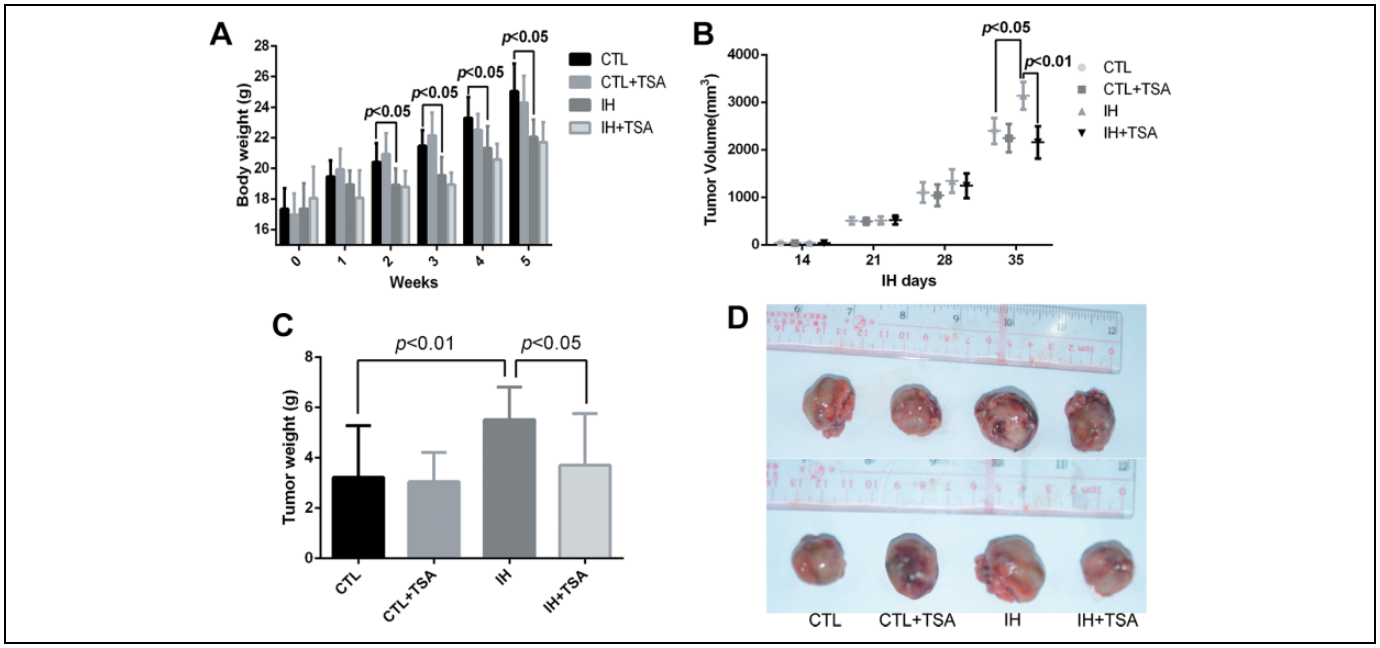

Figure 1. TSA injection significantly reduces IH-induced increases in tumor volume and tumor weight. A, The body weight of mice was measured at the indicated weeks after IH administration in the CTL, CTL + TSA, IH, and IH + TSA groups. B, Tumor volume in the indicated groups was measured at 14, 21, 28, and 35 days after IH administration. C, Tumor weight in the indicated groups was estimated in the fifth week after IH. Data represent the mean of independent assays performed in triplicate. *P* values are noted above the corresponding groups. D, The representative tumor size in each group was photographed. CTL indicates control; IH, intermittent hypoxia; TSA, sodium tanshinone IIA sulfonate.

AOBS; Leica) at a 400× magnification. Both TUNEL-positive cells and total cells were counted in 5 sections of each group. The apoptotic rate was calculated as follows: TUNEL-positive cell number/total cell number × 100%.

Statistical Analysis

GraphPad Prism software 5.0 (GraphPad Software, Inc.) was conducted to analyze the data. All data are presented as the mean ± standard deviation and were compared using an analysis of variance followed by the Fisher exact test. A *P* value less than .05 indicated statistical significance.

Results

TSA Injection Significantly Reduces IH-Induced Elevation in Tumor Volume and Tumor Weight

During the 5 weeks of the experiment, no mouse died and no severe TSA-related adverse event occurred in any group. Mice administered IH clearly lost body weight in weeks 2 to 5 ($P < .05$) compared with the CTL group (Figure 1A). However, both tumor volume ($p < .05$) and tumor weight ($P < .001$) in the IH group were obviously higher than those in the CTL group in the fifth week (Figure 1B-D). Sodium tanshinone IIA sulfonate injection (IH + TSA group) significantly reduced IH-induced increases in tumor volume ($P < .01$) and tumor weight ($P < .05$) compared with the IH group (Figure 1B-D).

TSA Effectively Attenuates IH-Induced Tumor Oxidative Stress

To evaluate the tumor oxidative state, serum levels of MDA and SOD were detected using colorimetric and enzymatic assays. Malondialdehyde serum level in the IH group was significantly higher than that in the CTL group ($P < .05$). Notably, TSA injection (IH + TSA group) significantly decreased MDA level compared with the IH group ($P < .01$). On the other hand, SOD serum level in the IH group was significantly reduced compared to the CTL group ($P < .01$). TSA injection (IH + TSA group) significantly increased SOD level compared with the IH group ($P < .01$; Figure 2).

IH Administration Increases HIF-1α Expression in LLC

Hypoxia-induced factor-1α gene and protein expressions in LLC tumors were markedly increased in the IH group compared with the CTL group ($P < .001$). However, TSA injection did not attenuate the IH-induced elevation of HIF-1α expression in either the CTL or IH group ($P > .05$; Figure 3).

TSA Significantly Promotes Tumor Apoptosis

Apoptotic factors BAX and cleaved caspase-3 were detected in the LLC tumor samples by Western blot analysis. Intermittent hypoxia administration (IH group) significantly decreased the protein expression of both BAX and cleaved caspase-3 ($P < .001$). Interestingly, TSA injection (IH + TSA group)

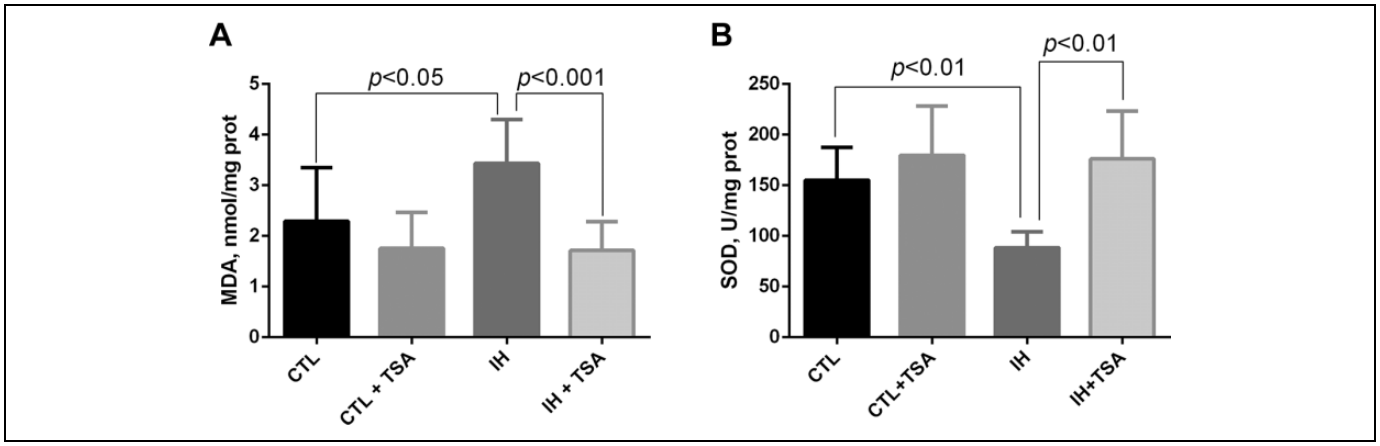

Figure 2. TSA effectively attenuates IH-induced tumor oxidative stress. A, Serum levels of MDA and B, SOD in the indicated groups were detected in the fifth week after IH administration using colorimetric and enzymatic assays. Data represent the mean of independent experiments. *P* values are noted above the corresponding groups. CTL indicates control; IH, intermittent hypoxia; MDA, malondialdehyde; SOD, superoxide dismutase; TSA, sodium tanshinone IIA sulfonate.

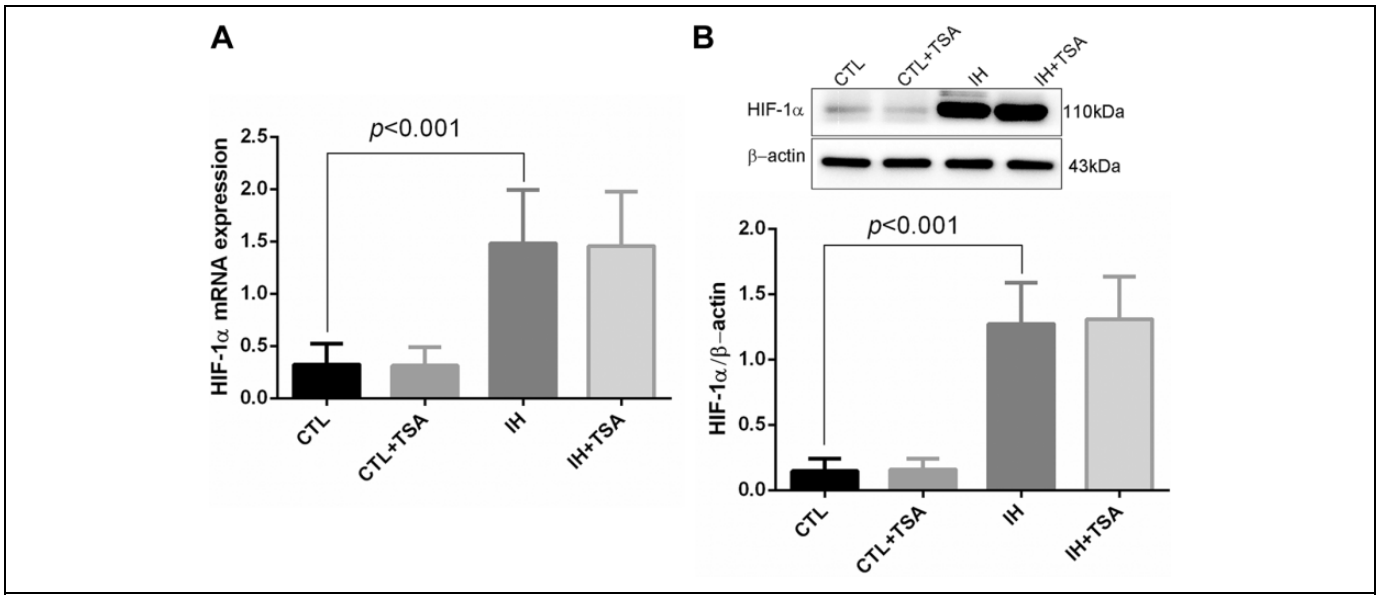

Figure 3. IH administration increases HIF-1α expression in LLC-implanted mice. HIF-1α mRNA and protein expression was analyzed by qRT-PCR (A) and Western blotting (B) in LLC tumor samples in the indicated groups. β-actin was used as the endogenous reference. Data represent the mean of independent experiments performed in triplicate. *P* values are noted above the corresponding groups. CTL indicates control; HIF-1α, hypoxia-inducible factor-1 α; IH, intermittent hypoxia; LLC, Lewis lung carcinoma; RT-PCR, real-time polymerase chain reaction; TSA, sodium tanshinone IIA sulfonate.

significantly attenuated the IH-induced decrease of BAX and cleaved caspase-3 ($P < .001$; Figure 4A and B). Further detection of apoptosis in the LLC tumors by TUNEL staining showed that TSA injection (IH + TSA group) noticeably promoted apoptotic activity compared with the IH group ($P < .001$; Figure 4C).

Signaling Pathways Underlying the Anticancer Activity of TSA in LLC

Western blot analysis showed that Nrf2 protein expression was downregulated in the IH group compared with the CTL group ($P < .01$). However, TSA treatment significantly reversed the IH-induced decrease of Nrf2 (Figure 5; $P < .01$). By contrast, the mean *p*-NF-κB p65 level was clearly upregulated after IH treatment (IH group) compared with the CTL group ($P < .001$). Notably, TSA treatment significantly attenuated the IH-induced increase of *p*-NF-κB p65 (Figure 6; $P < .001$).

Discussion

Recent studies have indicated that IH administration promotes tumor growth.[15-17,19] Our previous study confirmed this

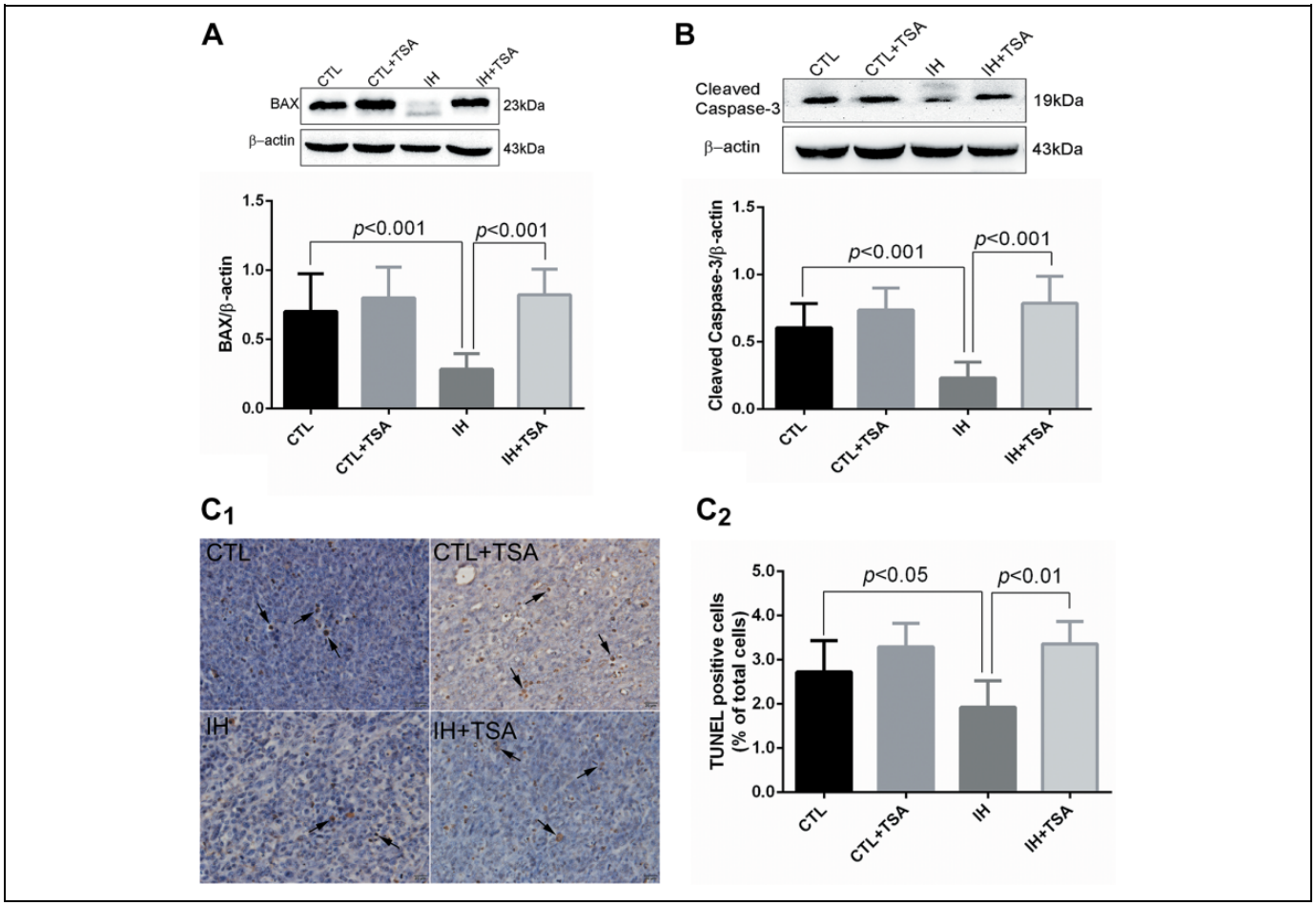

Figure 4. Pro-apoptotic activity of TSA in tumor samples from LLC-implanted mice. Protein expression of BAX (A) and cleaved caspase-3 (B) was analyzed by Western blotting of LLC tumor samples in the indicated groups. Upper panels are representative images; lower panels of the graphs are a summary of independent experiments performed in triplicate. β-actin was employed as the endogenous reference. Representative images of apoptotic cells stained with TUNEL are shown in C_1. Summary of independent TUNEL assays performed in triplicate are shown in C_2. *P* values are noted above the corresponding groups. BAX indicates B-cell lymphoma 2-associated protein X; CTL, control; IH, intermittent hypoxia; LLC, Lewis lung carcinoma; TSA, sodium tanshinone IIA sulfonate; TUNEL, terminal deoxynucleotidyl transferase dUTP nick-end labeling.

finding and showed that IH treatment clearly increased LLC growth in mice.[20,22] Here, we showed that not only the size but also the weight of the implanted LLC tumor significantly increased in the IH group. Excessive oxidative stress is one pathological characteristic of cancer. Growing data have shown that overproduction of ROS can significantly accelerate tumor cell proliferation, angiogenesis, invasiveness, and metastasis.[31] Antioxidant therapy can suppress ROS-driven tumor progression and metastasis,[32] although over-oxidative stress could be a strategy of anticancer therapy.[33] Studies have indicated that IH (a hallmark feature of OSA) upregulates oxidative stress in tumor models.[15-17,19] The underlying molecular mechanism of IH-induced tumor growth was investigated in this study in an LLC-implanted mouse model, showing that IH-treatment enhanced MDA levels but declined SOD activity in LLC-implanted mice, suggesting that excessive oxidative stress might be a mechanism to facilitate tumor growth.

Hypoxia-induced factor-1α and other pro-inflammatory factors (eg, activator protein 1, p53, NF-κB) are regulated by redox, in which Nrf2, SOD, and redox factor-1 play crucial roles in many pathological processes.[34,35] Our data revealed that IH administration markedly decreased Nrf2 expression, accompanied by an increase in NF-κB and HIF-1α, indicating that inhibition of Nrf2 and upregulation of NF-κB and HIF-1α might be a mechanism of IH-induced tumor growth. Indeed, Zhou *et al*[36] found that overexpression of Nrf2 in the heart increased resistance to IH-induced injury, whereas knockout (KO) of Nrf2 resulted in high sensitivity to IH-induced injury in Nrf2-KO mice. These data suggest that Nrf2 acts as an anti-oxidative factor during IH. In an IH-treated rat model, Zhang *et al*[37] reported that both NF-κB and HIF-1α expression were significantly upregulated in the heart after 6 weeks of IH treatment. This finding indicates that NF-κB and HIF-1α play important roles in IH-induced heart injury. Our data showed similar findings in tumorigenesis.

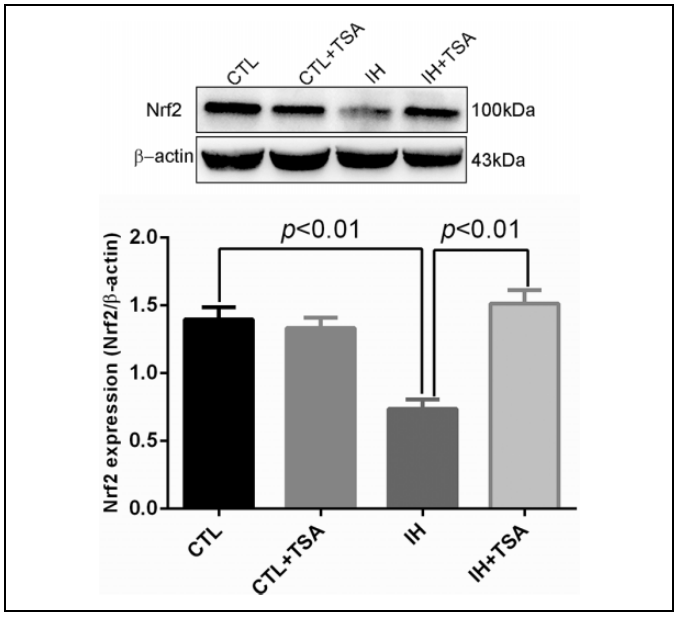

Figure 5. TSA attenuates the IH-induced decrease of Nrf2 protein expression. Western blot analysis of Nrf2 from LLC tumor samples in the indicated groups was conducted. β-actin was employed as the endogenous reference. The upper panel is a representative Western blot image of Nrf2. The lower panel is a summary of independent experiments performed in triplicate in the indicated groups. *P* values are noted above the corresponding groups. CTL indicates control; IH, intermittent hypoxia; LLC, Lewis lung carcinoma; Nrf2, nuclear factor erythroid 2-related factor 2; TSA, sodium tanshinone IIA sulfonate.

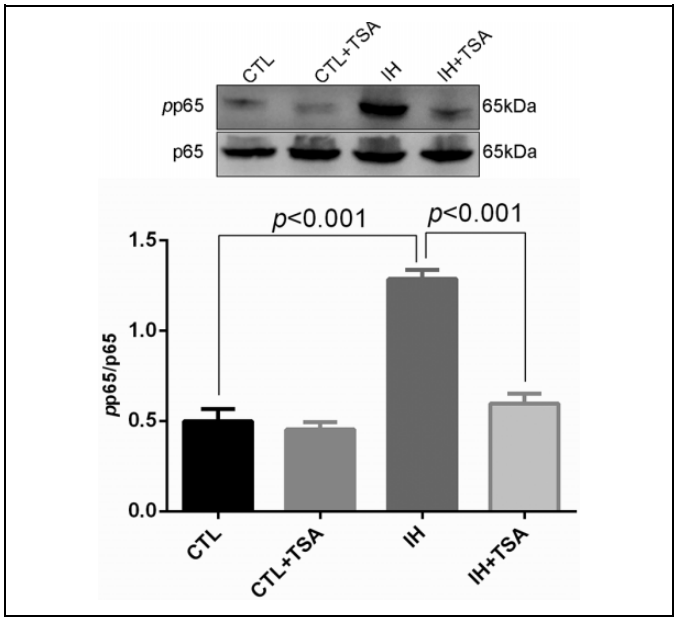

Figure 6. TSA attenuates the IH-induced upregulation of *p*-NF-κ protein expression. Western blot analysis of *p*-NF-κB p65 from LLC tumor samples in the indicated group was conducted. Total p65 was employed as the p65 loading reference. The upper panel is a representative Western blot image of *p*-NF-κB p65; the lower panel is a summary of independent experiments performed in triplicate in the indicated groups. *P* values are noted above the corresponding groups. CTL indicates control; IH, intermittent hypoxia; LLC, Lewis lung carcinoma; NF-κB, nuclear factor kappa B; TSA, sodium tanshinone IIA sulfonate.

Sodium tanshinone IIA sulfonate is an extract of the Chinese herb *S miltiorrhiza*. Its anti-inflammatory and antioxidant activities are widely used in clinical practice to treat a large number of cardiovascular and organ system diseases.[3,25] More recently, experimental studies have illustrated that TSA exerts anticancer effects through antioxidant activity and apoptosis regulation.[6,7] These findings were confirmed in our study as well. Sodium tanshinone IIA sulfonate treatment suppressed IH-induced oxidative stress in the LLC-implanted tumor model through downregulation of NF-κB and elevation of both Nfr2 and SOD expression, but not of HIF-1α. Further studies are needed to determine how IH and TSA influence SOD production and affect the expression of those transcription factors. Numerous antioxidant processes involve activation of Nrf2-related signaling pathways.[38-40] Lower expression of Nrf2 has been observed in OSA patients and in IH animal models.[41,42] Our results are in accordance with previous studies showing that Nrf2 expression is downregulated in IH-treated LLC-implanted mice, which is attenuated by TSA treatment.

NF-κB plays a crucial role in inflammation, oxidative stress, and apoptosis.[43,44] Previous studies have shown the importance of NF-κB in OSA and IH. Israel *et al*[45] showed that NF-κB is activated in children with OSA. Another study by Ryan and coworkers[46] showed that NF-κB-dependent gene expression was increased in OSA patients. Experimental studies have demonstrated that NF-κB is activated after exposing in mice or cells to IH.[24,47] Sodium tanshinone IIA sulfonate may protect against immune-mediated liver injury via the NF-κB signaling pathway in mice.[48] This study showed the activation (phosphorylation) of NF-κB in IH-treated LLC-implanted mice, which was attenuated by TSA administration.

A large number of studies have demonstrated the correlation between Nrf2 and NF-κB[49-51]; however, the precise effects and underlying molecular mechanisms of Nrf2 and NF-κB in IH-induced oxidative stress and apoptosis are still unknown. Our previous study suggested that HIF-1α is increased by IH treatment.[22] Here, we showed that increased HIF-1α expression was not reversed by TSA treatment. This finding conflicts with a previous study showing that TSA suppressed HIF-1α expression *in vitro* and *in vivo*.[52,53] Whether this discrepancy can be attributed to the different study subjects and different pretreatment conditions needs further studies.

Apoptosis is a natural mechanism for removing aged or damaged cells from the body. In cancer, however, the activation of antiapoptotic systems leads to loss of control of cell proliferation.[54] In this study, IH treatment markedly induced the growth of implanted LLC tumors, accompanied by decreased apoptosis (ie, decrease in BAX and cleaved caspase-3 expression, increase in TUNEL staining). Previous studies have shown that TSA has proapoptotic activity in several cancer cell lines and thus may be a potential therapy for cancer. The present study also revealed the antiapoptotic

activity of TSA in IH-treated LLC-implanted mice. Interestingly, TSA increased tumor apoptosis with IH treatment.

There were several limitations of this study. First, only 1 dose (10 mg/kg) of TSA was administered to the mice, so the dose–effect relationship was not evaluated. Second, only tumor oxidative stress and apoptotic levels were measured to evaluate the therapeutic effects of TSA on IH. Other properties including tumor cell proliferation, migration, and invasion should be assessed in future studies. Third, we observed discrepant expression of Nrf2 and *p*-NF-κB among groups. Expression of *p*-NF-κB and its inhibitor in both the cytoplasm and nucleus was not detected in this study. RNA interference (small interfering RNA against Nrf2 or NF-κB) or DNA binding experiments (electrophoretic mobility shift assay) are required to elucidate the role of Nrf2/NF-κB[51] in the effect of TSA on the behavior of tumors under IH.

Conclusion

This study showed that IH promoted oxidative stress and inhibited apoptosis in LLC-implanted mice. Improvements of IH-induced oxidative stress and apoptosis by TSA may involve the Nrf2/NF-κB signaling pathway. The results of this study indicate that TSA may be an adjunctive therapy for OSA patients with cancer.

Authors' Note

X.B.Z., X.Y.C., P.S., and X.M.S contributed equally to this work. X.B.Z., X.Y.C., and H.Q.Z conceived and designed the study. Collection and assembly of data were done by X.M.S., and M.W. X.B.Z., X.M.S., X.B.L., and H.Q.Z aided in data analysis and interpretation. All authors contributed to the writing of the manuscript. All authors contributed to the final approval of the manuscript.

Declaration of Conflicting Interests

The author(s) declared no potential conflicts of interest with respect to the research, authorship, and/or publication of this article.

Funding

The author(s) disclosed receipt of the following financial support for the research, authorship, and/or publication of this article: This work was supported by grant 2018-2-65 for Youth Research Fund from Fujian Provincial Health Bureau, and grant 2018J01393 for Fund from Natural Science Foundation of Fujian Province, China.

ORCID iD

Xiao-Bin Zhang https://orcid.org/0000-0002-5155-8560

References

1. Hu Q, Wei B, Wei L, et al. Sodium tanshinone IIA sulfonate ameliorates ischemia-induced myocardial inflammation and lipid accumulation in Beagle dogs through NLRP3 inflammasome. *Int J Cardiol*. 2015;196(7):183-192.
2. Qian C, Ren Y, Xia Y. Sodium tanshinone IIA sulfonate attenuates hemorrhagic shock-induced organ damages by nuclear factor-kappa B pathway. *J Surg Res*. 2017;209(3):145-152.
3. Wei B, Li WW, Ji J, Hu QH, Ji H. The cardioprotective effect of sodium tanshinone IIA sulfonate and the optimizing of therapeutic time window in myocardial ischemia/reperfusion injury in rats. *Atherosclerosis*. 2014;235(2):318-327.
4. Dong Y, Morris-Natschke SL, Lee KH. Biosynthesis, total syntheses, and antitumor activity of tanshinones and their analogs as potential therapeutic agents. *Nat Prod Rep*. 2011;28(3):529-542.
5. Yun SM, Jung JH, Jeong SJ, Sohn EJ, Kim B, Kim SH. Tanshinone IIA induces autophagic cell death via activation of AMPK and ERK and inhibition of mTOR and p70 S6 K in KBM-5 leukemia cells. *Phytother Res*. 2014;28(3):458-464.
6. Zhang Y, Wei RX, Zhu XB, Cai L, Jin W, Hu H. Tanshinone IIA induces apoptosis and inhibits the proliferation, migration, and invasion of the osteosarcoma MG-63 cell line in vitro. *Anticancer Drugs*. 2012;23(2):212-219.
7. Liu F, Yu G, Wang G, et al. An NQO1-initiated and p53-independent apoptotic pathway determines the anti-tumor effect of tanshinone IIA against non-small cell lung cancer. *PLoS One*. 2012;7(7): e42138.
8. Li Q, Wang Y, Feng N, Fan Z, Sun J, Nan Y. Novel polymeric nanoparticles containing tanshinone IIA for the treatment of hepatoma. *J Drug Target*. 2008;16(10):725-732.
9. Chen J, Shi DY, Liu SL, Zhong L. Tanshinone IIA induces growth inhibition and apoptosis in gastric cancer in vitro and in vivo. *Oncol Rep*. 2012;27(2):523-528.
10. Young T, Peppard PE, Gottlieb DJ. Epidemiology of obstructive sleep apnea: a population health perspective. *Am J Respir Crit Care Med*. 2002;165(9):1217-1239.
11. Heinzer R, Vat S, Marques-Vidal P, et al. Prevalence of sleep-disordered breathing in the general population: the HypnoLaus study. *Lancet Respir Med*. 2015;3(4):310-318.
12. Peppard PE, Young T, Barnet JH, Palta M, Hagen EW, Hla KM. Increased prevalence of sleep-disordered breathing in adults. *Am J Epidemiol*. 2013;177(9):1006-1014.
13. Jordan AS, McSharry DG, Malhotra A. Adult obstructive sleep apnoea. *Lancet*. 2014;383(9918):736-747.
14. Lai MC, Lin JG, Pai PY, et al. Protective effect of salidroside on cardiac apoptosis in mice with chronic intermittent hypoxia. *Int J Cardiol*. 2014;174(3):565-573.
15. Marshall NS, Wong KK, Cullen SR, Knuiman MW, Grunstein RR. Sleep apnea and 20-year follow-up for all-cause mortality, stroke, and cancer incidence and mortality in the Busselton Health Study cohort. *J Clin Sleep Med*. 2014;10(4):355-362.
16. Martinez-Garcia MA, Campos-Rodriguez F, Duran-Cantolla J, et al. Obstructive sleep apnea is associated with cancer mortality in younger patients. *Sleep Med*. 2014;15(7):742-748.
17. Almendros I, Montserrat JM, Ramirez J, et al. Intermittent hypoxia enhances cancer progression in a mouse model of sleep apnoea. *Eur Respir J*. 2012;39(1):215-217.
18. Almendros I, Montserrat JM, Torres M, et al. Intermittent hypoxia increases melanoma metastasis to the lung in a mouse model of sleep apnea. *Respir Physiol Neurobiol*. 2013;186(3):303-307.
19. Almendros I, Wang Y, Becker L, et al. Intermittent hypoxia-induced changes in tumor-associated macrophages and tumor malignancy in a mouse model of sleep apnea. *Am J Respir Crit Care Med*. 2014;189(5):593-601.

20. Zhang XB, Yang YY, Zeng Y, et al. Anti-tumor effect of endostatin in a sleep-apnea mouse model with tumor. *Clin Transl Oncol*. 2019;21(5):572-581.
21. National Research Concil (US) Committee for the Update of the Guide for the Care and Use of Laboratory Animals. Guide for the Care and Use of Laboratory Animals. National Academies Press (US); 2011.
22. Huang MH, Zhang XB, Wang HL, et al. Intermittent hypoxia enhances the tumor programmed death ligand 1 expression in a mouse model of sleep apnea. *Ann Transl Med*. 2019;7(5):97.
23. Zhang XB, Cai JH, Yang YY, et al. Telmisartan attenuates kidney apoptosis and autophagy-related protein expression levels in an intermittent hypoxia mouse model. *Sleep Breath*. 2019;23(1): 341-348.
24. Zhang XB, Zeng YM, Chen XY, Zhang YX, Ding JZ, Xue C. Decreased expression of hepatic cytochrome P450 1A2 (CYP1A2) in a chronic intermittent hypoxia mouse model. *J Thorac Dis*. 2018;10(2):825-834.
25. Xu QQ, Xu YJ, Yang C, et al. Sodium tanshinone IIA sulfonate attenuates scopolamine-induced cognitive dysfunctions via improving cholinergic system. *Biomed Res Int*. 2016;2016(2): 9852536.
26. Wang J, Jiang Q, Wan L, et al. Sodium tanshinone IIA sulfonate inhibits canonical transient receptor potential expression in pulmonary arterial smooth muscle from pulmonary hypertensive rats. *Am J Respir Cell Mol Biol*. 2013;48(1):125-134.
27. Jiang X, Chen Y, Zhu H, et al. Sodium tanshinone IIA sulfonate ameliorates bladder fibrosis in a rat model of partial bladder outlet obstruction by inhibiting the TGF-beta/Smad pathway activation. *PLoS One*. 2015;10(6):e0129655.
28. Jiao F, Qu Y, Zhou G, et al. Modulation of oxidative stress by functionalized fullerene materials in the lung tissues of female C57/BL mice with a metastatic Lewis lung carcinoma. *J Nanosci Nanotechnol*. 2010;10(12):8632-8637.
29. Li X, Zhu F, Jiang J, et al. Synergistic antitumor activity of withaferin A combined with oxaliplatin triggers reactive oxygen species-mediated inactivation of the PI3K/AKT pathway in human pancreatic cancer cells. *Cancer Lett*. 2015;357(1): 219-230.
30. Ji H, Wu L, Ma X, Ma X, Qin G. The effect of resveratrol on the expression of AdipoR1 in kidneys of diabetic nephropathy. *Mol Biol Rep*. 2014;41(4):2151-2159.
31. Nishikawa M. Reactive oxygen species in tumor metastasis. *Cancer Lett*. 2008;266(1):53-59.
32. Goh J, Enns L, Fatemie S, et al. Mitochondrial targeted catalase suppresses invasive breast cancer in mice. *BMC Cancer*. 2011; 11(2):191.
33. Kim SJ, Kim HS, Seo YR. Understanding of ROS-inducing strategy in anticancer therapy. *Oxid Med Cell Longev*. 2019;2019(4): 5381692.
34. Zhang R, Chae S, Lee JH, Hyun JW. The cytoprotective effect of butin against oxidative stress is mediated by the up-regulation of manganese superoxide dismutase expression through a PI3K/Akt/Nrf2-dependent pathway. *J Cell Biochem*. 2012;113(6): 1987-1997.
35. Tell G, Quadrifoglio F, Tiribelli C, Kelley MR. The many functions of APE1/Ref-1: not only a DNA repair enzyme. *Antioxid Redox Signal*. 2009;11(3):601-620.
36. Zhou S, Yin X, Jin J, et al. Intermittent hypoxia-induced cardiomyopathy and its prevention by Nrf2 and metallothionein. *Free Radic Biol Med*. 2017;112:224-239.
37. Zhang J, Zheng L, Cao J, Chen B, Jin D. Inflammation induced by increased frequency of intermittent hypoxia is attenuated by tempol administration. *Braz J Med Biol Res*. 2015;48(12):1115-1121.
38. Qin X, Meghana K, Sowjanya NL, et al. Embelin attenuates cisplatin-induced nephrotoxicity: involving inhibition of oxidative stress and inflammation in addition with activation of Nrf-2/Ho-1 pathway. *Biofactors*. 2019;45(3):471-478.
39. Sobeh M, Petruk G, Osman S, et al. Isolation of myricitrin and 3,5-di-O-methyl gossypetin from syzygium samarangense and evaluation of their Involvement in protecting keratinocytes against oxidative stress via activation of the Nrf-2 pathway. *Molecules*. 2019;24(9):8.
40. Sun Q, Wu Y, Zhao F, Wang J. Maresin 1 ameliorates lung ischemia/reperfusion injury by suppressing oxidative stress via activation of the Nrf-2-mediated HO-1 signaling pathway. *Oxid Med Cell Longev*. 2017;2017(2):9634803.
41. Zhou L, Ouyang R, Luo H, et al. Dysfunction of Nrf2-ARE signaling pathway: potential pathogenesis in the development of neurocognitive impairment in patients with moderate to severe obstructive sleep apnea-hypopnea syndrome. *Oxid Med Cell Longev*. 2018;2018(1):3529709.
42. Zhou S, Wang J, Yin X, et al. Nrf2 expression and function, but not MT expression, is indispensable for sulforaphane-mediated protection against intermittent hypoxia-induced cardiomyopathy in mice. *Redox Biol*. 2018;19(1):11-21.
43. Mangali S, Bhat A, Udumula MP, Dhar I, Sriram D, Dhar A. Inhibition of protein kinase R protects against palmitic acid-induced inflammation, oxidative stress, and apoptosis through the JNK/NF-kB/NLRP3 pathway in cultured H9C2 cardiomyocytes. *J Cell Biochem*. 2019;120(3):3651-3663.
44. Kin H, Wang NP, Mykytenko J, et al. Inhibition of myocardial apoptosis by postconditioning is associated with attenuation of oxidative stress-mediated nuclear factor-kappa B translocation and TNF alpha release. *Shock*. 2008;29(6):761-768.
45. Israel LP, Benharoch D, Gopas J, Goldbart AD. A pro-inflammatory role for nuclear factor kappa B in childhood obstructive sleep apnea syndrome. *Sleep*. 2013;36(12): 1947-1955.
46. Ryan S, Taylor CT, McNicholas WT. Predictors of elevated nuclear factor-kappa B-dependent genes in obstructive sleep apnea syndrome. *Am J Respir Crit Care Med*. 2006;174(7): 824-830.
47. Greenberg H, Ye X, Wilson D, Htoo AK, Hendersen T, Liu SF. Chronic intermittent hypoxia activates nuclear factor-kappaB in cardiovascular tissues in vivo. *Biochem Biophys Res Commun*. 2006;343(2):591-596.
48. Xu Y, Feng D, Wang Y, Lin S, Xu L. Sodium tanshinone IIA sulfonate protects mice from ConA-induced hepatitis via inhibiting NF-kappaB and IFN-gamma/STAT1 pathways. *J Clin Immunol*. 2008;28(5):512-519.

49. Ziady AG, Sokolow A, Shank S, et al. Interaction with CREB binding protein modulates the activities of Nrf2 and NF-kappaB in cystic fibrosis airway epithelial cells. *Am J Physiol Lung Cell Mol Physiol*. 2012;302(11): L1221-L1231.
50. Liu GH, Qu J, Shen X. NF-kappaB/p65 antagonizes Nrf2-ARE pathway by depriving CBP from Nrf2 and facilitating recruitment of HDAC3 to MafK. *Biochim Biophys Acta*. 2008;1783(5): 713-727.
51. Wang Z, Han G, Liu Q, Zhang W, Wang J. Silencing of PYGB suppresses growth and promotes the apoptosis of prostate cancer cells via the NFkappaB/Nrf2 signaling pathway. *Mol Med Rep*. 2018;18(4):3800-3808.
52. Guan R, Wang J, Li Z, et al. Sodium tanshinone IIA sulfonate decreases cigarette smoke-induced inflammation and oxidative stress via blocking the activation of MAPK/HIF-1alpha signaling pathway. *Front Pharmacol*. 2018;9: 263.
53. Kim JY, Song JJ, Kwon BM, Lee JD. Tanshinone IIA exerts antitumor activity against vestibular schwannoma cells by inhibiting the expression of hypoxia-inducible factor-1alpha. *Mol Med Rep*. 2015;12(3):4604-4609.
54. Mohammad RM, Muqbil I, Lowe L, et al. Broad targeting of resistance to apoptosis in cancer. *Semin Cancer Biol*. 2015; 35(suppl):S78-S103.